Macromolecules

Volume 31, Number 5 March 10, 1998

Liquid Crystal Polymers Containing Ni(II), Pd(II), or VO(II) in the Main Chain

Ugo Caruso,* Antonio Roviello, Augusto Sirigu, and Carmela Troise

Dipartimento di Chimica dell'Università degli Studi "Federico II", Via Mezzocannone, 4-80134 Napoli, Italy

Received February 11, 1997; Revised Manuscript Received December 2, 1997

ABSTRACT: The synthesis and the phase behavior of a homologous series of polymers of 4,4′-[1,12-dodecanediylbis(oxy)]bis(benzoic acid) with bis[*N*-[[2,4-dihydroxyphenyl]methylene]alkylamino]nickel(II), -palladium(II) and -oxovanadium(II) are reported. Calorimetric and X-ray diffraction data and dynamic viscosity measurements are consistent with the occurrence of nematic mesomorphism for all polymers. The nematic phase, which is monotropic for some of the nickel-containing polymers, is comparatively more stable for those containing palladium. Polymers containing the oxovanadium group show also enantiotropic smectic mesomorphism. The mesophase properties of ligand systems are also discussed.

Introduction

In the past decade several metal-containing liquid crystal (LC) polymers have been prepared and characterized.[1] Interest in this class of mesogens arises not only from the chemical and structural versatility, which allows us to obtain new and peculiar molecular geometries, for example, by the coordination of suitable ligands to transition metal ions, but also from the possibility of having an effect upon dielectric, chromatic, and magnetic properties of the materials. While LC polymers containing complexed copper have been largely studied,[1] only a few examples of polymers containing other coordinated metal ions are known. In particular, for Ni(II)-containing LC polymers, no data concerning linear polymers ar available, while some cross-linked polymers have been reported by Hanabusa et al.[2,3] As to Pd(II)-containing LC polymers, a few cases have been reported concerning liotropic polymers,[4] side chain orthopalladate polysiloxanes,[5] and one single example of linear polymer.[6] Finally, notwithstanding the good magnetic properties of oxovanadium complexes (a magnetic moment at room temperature of the order of 1.6 μ_B has been reported for salicyladiminate oxovanadium complexes[7]) and the possibility, experimentally assessed for low-molecular-weight complexes,[8−10] of building molecular structures compatible with the onset of liquid crystallinity, a single example of a liquid-crystal polymer containing coordinated oxovanadium groups has been reported by Serrano and co-workers.[11] These authors synthesized a series of hydroxy-funzionalized liquid-crystalline polyazomethines which were subsequently cross-linked by oxovanadium complexation of the salicylaldiminate cores. The cross-linked polymers exhibit a nematic phase as the starting polyazomethines.

With the aim of increasing the available data on the relationships between liquid crystalline properties and the nature of the coordinated metal, we have synthesized polymers with the general formula

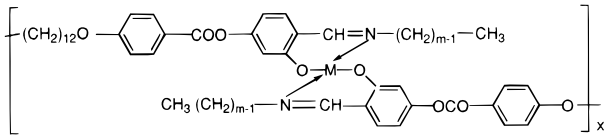

P12-mNM

with $m = 8-11$ for M = Pd, $m = 8-12$ for M = Ni, and $m = 6$, 8, and 10 for M = VO.

The phase behavior of these polymers has been investigated and compared also with that of a previously studied[12] class of analogous copper-containing liquid-crystal polymers.

Experimental Section

The three classes of polymers have been prepared following different routes.

* To whom correspondence should be addressed. E-mail: Caruso@chemna.dichi.unina.it.

S0024-9297(97)00187-3 CCC: $15.00
Published on Web 02/13/1998

Scheme 1

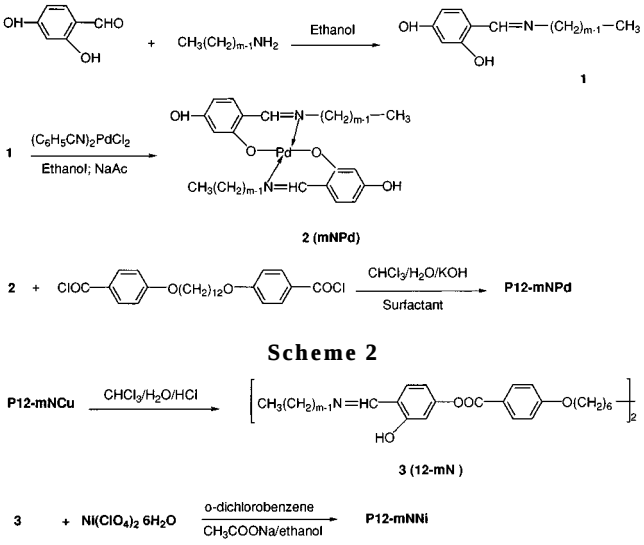

Scheme 2

Palladium-containing polymers have been prepared in a way analogous to that reported in refs 6 and 12 for the synthesis of the homologous polymers containing Cu(II) or Pd(II). The procedure followed for the preparation of P12-11NPd, taken as an example, is reported here with some detail (Scheme 1). However, it may be easily extended as a general scheme.

In the first step 3.6 g of *n*-undecylamine is added to a solution of 3.0 g of 2,4- dihydroxybenzaldehyde in 70 mL of boiling absolute ethanol to produce imine **1**. To this solution, cooled at room temperature, 4.3 g of $PdCl_2(C_6H_5CN)_2$ and 1.5 g of KOH are added under nitrogen atmosphere. The solution is kept at room temperature for 3 h. Crystalline **2**, which progressively precipitates, is filtered and recrystallized from methanol (yield 57%). Polymerization was performed by interfacial reaction. A solution of 2.176 g of 4,4′-[1,12-dodecanediylbis(oxy)]bis(benzoic acid chloride), prepared from the corresponding bis(benzoic acid) according to a literature method,[13] in 70 mL of chloroform is added under vigorous stirring to a solution of 3.090 g of **2**, 0.789 of KOH in 110 mL of water, and 0.875 of tetrabutylammonium hydrogen sulfate as a surfactant. After 10 min of reaction, 100 mL of chloroform is added and the organic phase is separated. After three extractions with water, to remove water-soluble residues, the chloroform solution is dried over Na_2SO_4 and added to 300 mL of hot ethanol. Polymer precipitates as a yellow solid and is washed twice with hot ethanol (yield 43%).

Nickel-containing polymers have been synthesized according to the following route (Scheme 2):

Hereinafter the detailed procedure of the synthesis of the polymer P12-8NNi is described:

To a solution of 9.0 g of polymer P12-8NCu, previously prepared following a method already described (ref 9), in 200 mL of chloroform is added a solution of 10 mL of 37% HCl dissolved in 200 mL of water at room temperature under stirring. The reaction proceeds for a few minutes until the green-brown color, typical of the polymer solution, disappears. The chloroformic phase is washed many times with water, dried over Na_2SO_4, concentrated, and added to 200 mL of ethanol. Compound 12-8N (diimine **3**, $m = 8$) precipitates as a yellow crystalline solid. A further crystallization is performed from a chloroform/ethanol solution (yield 85%). In the polymerization step 0.132 g of nickel perchlorate in 5 mL of absolute ethanol is added slowly at room temperature to a solution obtained by mixing 0.448 g of 12-8N in 20 mL of *o*-dichlorobenzene and 0.12 g of sodium acetate dissolved in 10 mL of absolute ethanol. The polymer precipitates readily as a green solid. Its purification is obtained by dissolution in 20 mL of hot *o*-dichlorobenzene followed by filtration and precipitation in hot *n*-hexane. Finally, the polymer is washed twice with boiling ethanol (yield 70%).

Chart 1

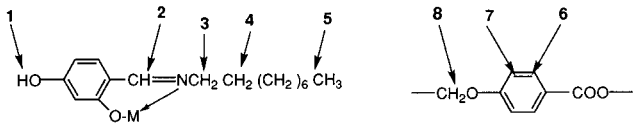

Table 1. Some Characteristic ^{1}H NMR Data of Intermediate and Polymer Compounds[a]

	1	2	3	4	5	6	7	8
9NPd	8.6s	7.7s	3.7t	1.7m	0.86m			
P12-9NPd		7.6	3.7	1.8	0.83	7.0	8.1	4.0
P12-9NNi		7.3	1.8	1.8	0.83	6.9	8.1	4.0
12-9N		8.3	3.6	1.7	0.88	7.2	8.1	4.0

[a] For atom labels, refer to Chart 1: δ (ppm).

Table 2. *m*NPd Thermodynamic Data Relative to Phase Transition[a]

m	T_{KK}	T_m	ΔH_m
8	93	220	87.7
9	178	212	92.6
10		206	81.0
11	162	206	74.2

[a] K = crystal phase; T_{KK} = solid−solid transition temperature (°C); the related transition enthalpy is very small and is not measured; T_m = melting temperature (°C); ΔH_m = melting enthalpy (J g^{-1}).

The synthetic path followed for the oxovanadium-containing polymers proceeds through the synthesis of a diimine ligand (Scheme 2) and a final interfacial reaction between the diimine and an oxovanadium salt. The synthesis of P12-8NVO is reported as an example.

Diimine **3** (1503 g) dissolved in 50 mL of chloroform is added, under vigorous stirring, to a water solution obtained dissolving 0.4324 g of oxovanadium sulfate (20% excess), 1.5 g of anhydrous sodium acetate, 0.154 g of tetrabutylammonium hydrogensulfate, and 0.03 g of potassium hydroxide in 100 mL of water. The pH of the reaction mixture was kept in the range 5−6. After a few minutes it was possible to note traces of a green gelatinous compound in the mixture. After 30 min of reaction, the pH was increased to 7 using sodium acetate, and after 2 more min the reaction was stopped. The chloroform solution was added to 200 mL of boiling ethanol containing 1 g of sodium acetate. P12-8NVO precipitated as a green-gray solid (yield 85%). The polymer was washed three times with boiling ethanol to extract lower molecular weight fractions. Vanadium content: P12-6NVO, 5.65% (calc 5.57%); P12-8NVO, 5.35% (calc 5.25%); P12-10NVO, 4.98% (calc 4.96%).

Following different synthetic routes has been necessary because the interfacial reaction of a dihydroxy metal complex with a diacid dichloride is viable only for palladium-containing polymers. This is mainly related to the instability of the Ni and VO analogues of compound **2** (Scheme 1) in alkaline aqueous solution. In addition, the high solubility of these compounds would make very difficult a proper purification with negative consequences on the molecular weights of Ni- and VO-containing polymers.

For the characterization of the phase behavior, differential scanning calorimetry (DSC), polarizing microscopy, and X-ray diffraction techniques were normally employed. For the DSC analysis, an indium-calibrated Perkin-Elmer DSC7 apparatus was utilized. Samples were examined under dry nitrogen atmosphere with a temperature scanning rate of 10 °C/min. The phase transition temperatures reported in the Discussion were measured at the maximum of the transition endotherms for polymers, while for low-molecular-weight compounds they are onset values. Optical observations were performed on a Zeiss Axioskop polarizing microscope equipped with a Mettler FP5 microfurnace. X-ray diffraction patterns were recorded by the photographic method utilizing a flat-film camera and the Ni-filtered Cu Kα radiation. Dynamic viscosity measure-

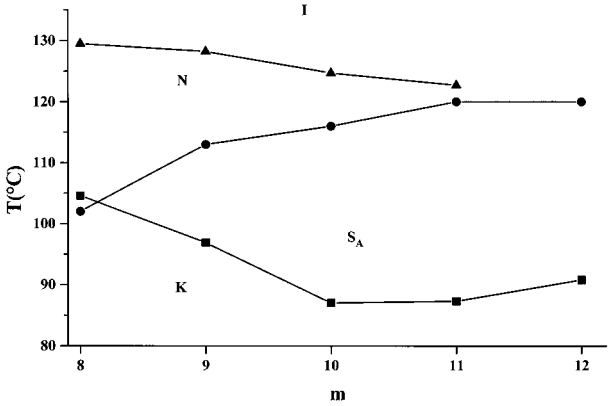

Figure 1. Phase transition temperatures for compounds 12-*m*N.

Table 3. Thermodynamic Data of Compounds 12-*m*N[a]

m	T_m	ΔH_m	T_l	ΔH_l	T_i	ΔH_i
8	104.6	93.1	102[b]	129.5	7.7	
9	96.9	93.3	113[b]	128.2	8.0	
10	87.0	50.8	116	0.81	124.7	7.0
11	87.3	46.4	120	*c*	122.7	13.7[c]
12[d]	90.8	51.1	120.0	12.9		

[a] T_m = melting temperature (°C); $T_l = S_A-N$ temperature (°C); T_i = isotropization temperature (°C); ΔH = enthalpic change (J g^{-1}). [b] Optical determination. [c] Referred to S_A-N-I. [d] KK at 73.2 ΔH = 21.3 and S_C-S_A at 81.5 °C by optical determination.

ments were performed utilizing a Rheometrics Recap 2 apparatus at an oscillatory frequency of 10 Hz. Measurements were performed at decreasing temperature (10 °C/min cooling rate) starting from the isotropic liquid. Glass transition temperatures were measured for polymer fibers using a Polymer Laboratories dynamic mechanical thermal analyzer (DMTA) under dry nitrogen atmosphere with a temperature scanning rate of 5 °C/min. The intrinsic viscosity of a chloroform solution of polymers was measured utilizing an Ubbelohde viscometer at 25.0 °C. The average molecular weight was measured by vapor pressure osmometry utilizing a Knauer apparatus; measurements were performed at 37.00 °C on a chloroform solution. FTIR spectrometry was performed on a Bruker IFS66 apparatus.

Results and Discussion

Intermediate Compounds. The compounds *m*NPd (compound **2** of Scheme 1), utilized to prepare the Pd-containing polymers, have been prepared according to a procedure already described in ref 6. Their ^{1}H NMR spectra are in agreement with the expected formulas; the most significant resonances (for the numbered atoms in Chart 1) are reported in Table 1 for 9NPd taken as an example. These compounds are nonmesogenic with rather high melting temperatures. Phase transition data are reported in Table 2.

The phase properties of imines 12-*m*N (compounds **3** of Scheme 2) are summarized in Figure 1 and some relevant thermodynamic data are collected in Table 3. The ^{1}H NMR spectra agree with the expected formulas; some significant resonances are reported in Table 2 for 12-9N taken as an example.

All these compounds exhibit mesomorphic behavior with polymorphism.

Compounds with $m = 8-11$ show a smectic A phase, morphologically characterized by coexisting fan and pseudoisotropic textures. At higher temperature, this morphology transforms into a very mobile schlieren characteristic of a nematic phase.

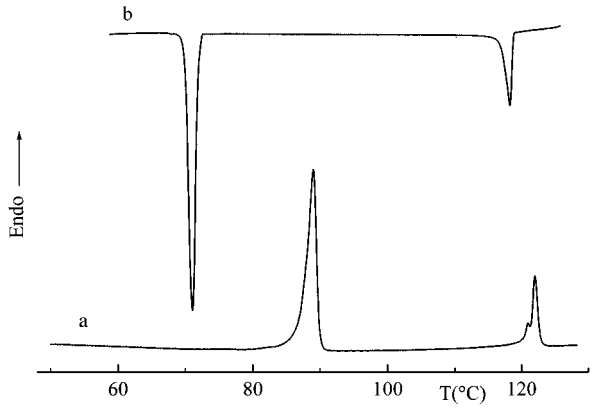

Figure 2. Thermal behavior of 12-11N: scan rate, 10 °C/min; (a) first heating run; (b) first cooling run.

Table 4. Thermodynamic Data of the Polymers P12-*m*NPd and P12-*m*NNi[a]

	P12-*m*NPd				P12-mNNi			
m	T_m	T_i	ΔH_i	$[\eta]$	T_m	T_i	ΔH_i	$[\eta]$
8	210	250	4.8	1.25	197	216	5.6	0.11[b]
9	212	246	4.8	1.68	210	214	5.7	0.12
10	180	232	4.7	1.33	155	206	5.5	0.20
11	194	227	4.4	2.10	197	197	5.5	0.63
12					198	195	5.4	0.45

[a] T_m = melting temperature (°C); T_i = isotropization temperature (°C); ΔH = enthalpic change (J g^{-1}); $[\eta]$ = limit viscosity number (dL g^{-1}) in chloroform at 25.0 °C. [b] Measured in *o*-dichlorobenzene at 40.0 °C.

The stability range of the nematic phase decreases with increasing *m*. The DSC behavior of compound 12-11N is reported in Figure 2 as an example. For this compound, the $S_A \rightarrow N$ and $N \rightarrow I$ transitions are not resolved. For $m = 12$, smectic mesomorphism takes over and the nematic phase is not observed. In addition to the smectic A phase, a monotropic smectic C phase is detectable, characterized by a broken-fan + schlieren texture. The S_C-S_A phase transition is optically observable at 81.5 °C with texture changes bringing the broken-fan to fan and the schlieren to pseudoisotropic. The S_A-N transition is monotropic for $m = 8$ and 9. The latter compound, when crystallized from the melt, forms a solid phase whose melting temperature may be brought up to 114 °C, that is, 1 °C higher than the $S_A \rightarrow N$ transition temperature. Analogous solid-state polymorphism is exhibited by 12-11N. Melt-crystallized samples melt as high as 110 °C. In this case, the smectic−nematic transition is truly enantiotropic. Data reported in Table 3 and in Figure 1 refer to solid phases as obtained by crystallization from solution. Solid-phase polymorphism, which involves also other compounds, being not central to our point, will not be dealt with any further.

The mesogenic properties of compounds 12-*m*N are presumably related to the presence of intramolecular hydrogen bonds between the hydroxy group and the imine nitrogen leading to a mesogenic group sterically similar to a 2,6-linked naphthyl moiety. Therefore, the molecular structure of this compounds is that of a twin mesogen. Consistently, isotropization enthalpies are comparatively high, as found in the literature for mesogens having a "dimeric" structure.[14]

A smectic periodicity of 68 ± 2 Å was measured by X-ray diffraction for 12-12N at 100 °C. This value is in good agreement with the molecular length of 12-12N

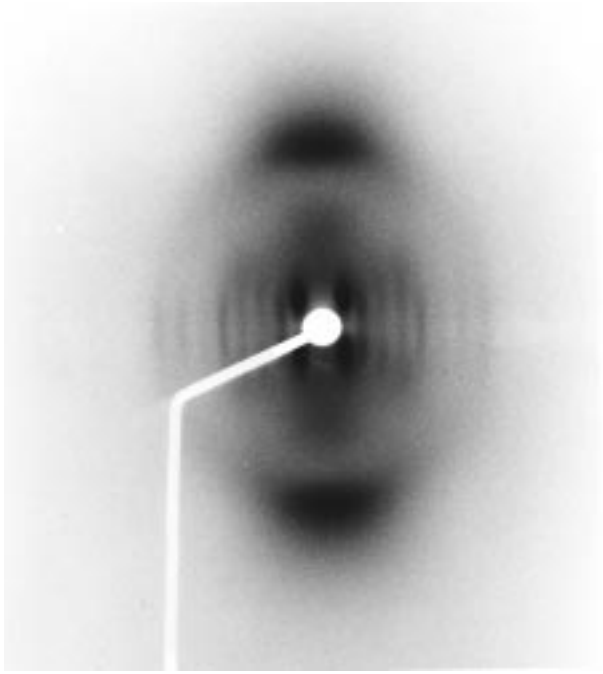

Figure 3. X-ray diffraction pattern recorded at room temperature for a melt-extruded fiber of P12-9NPd.

calculated for its most extended conformation and consistent with the S_A structure of the smectic phase as argued from textural features.

Pd-Containing Polymers. ^{1}H NMR spectra of polymers P12-*m*NPd agree with the expected formulas. Some significant resonances are reported in Table 2 for P12-9NPd taken as an example. All polymers have comparatively high molecular weights, as suggested by the intrinsic viscosity values, ranging from 1.25 to 2.10 dL g^{-1}, measured in chloroform solution at 25.0 °C. In accordance with that, vapor pressure osmometry experiments indicate average molecular weights exceeding the upper limit of applicability of the technique. As-prepared polymers are semicrystalline, as evidenced by differential scanning calorimetry and X-ray diffraction evidences. DSC analysis and optical observation at variable temperature coherently show that all polymers are mesomorphic with a stability range of the mesophases of about 40 °C. The thermodynamic data are reported in Table 4.

Samples kept for about 2 h above melting temperature undergo some chemical alteration. This did not allow a safe use of X-ray diffraction techniques for the determination of the nature of the mesomorphic state. However, its nematic structure could be ascertained by other means. The X-ray diffraction spectra recorded at room temperature for oriented fibers show their semicrystalline structure. However, for $m = 8$ and 9, the diffraction pattern of melt-extruded fibers undergoing rapid quenching in icy water is indicative of a mesomorphic structure of cybotactic nematic type. Figure 3 reports the diffraction pattern recorded at room temperature for P12-9NPd.

For $m = 10$ and 11, the nematic nature of the mesophase is clearly shown by the melt viscosity measurements as a function of temperature.

Figure 4 shows the melt viscosity curve recorded at decreasing temperatures for P12-11NPd with the superimposed DSC curve; both refer to a cooling rate of 10 °C/min. A sharp decrease of the melt viscosity,

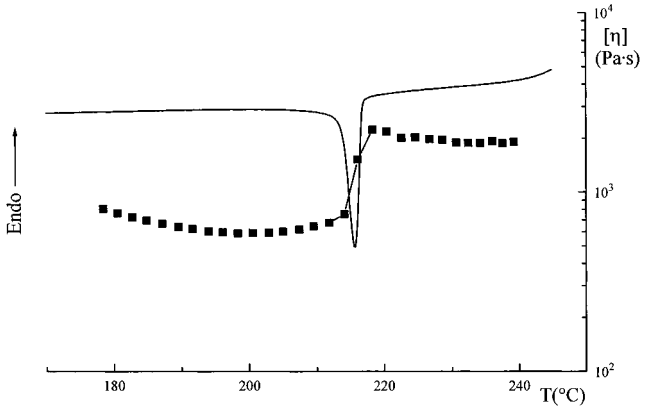

Figure 4. Melt viscosity (■) as a function of the temperature for the polymer P12-11NPd. Continuous line: DSC cooling curve.

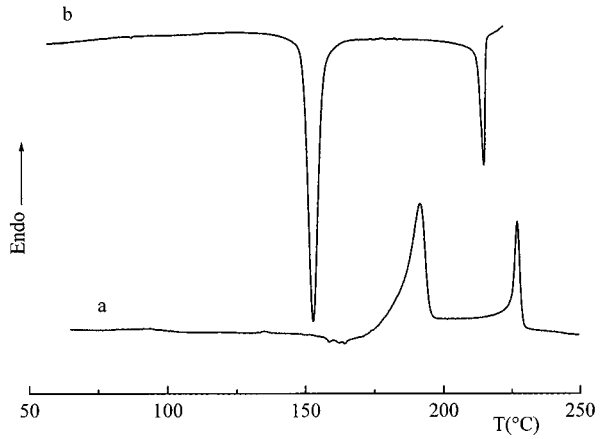

Figure 5. DSC curves for the polymer P12-11NPd: scan rate, 10 °C/min; (a) first heating run; (b) first cooling run.

typical of an isotropic−nematic transition, is detectable in correspondence to the liquid−liquid DSC exothermic transition. The thermal behavior of the same polymer is shown extensively in Figure 5. Furthermore, development of band structures is observed on molten samples sheared between two glasses under rapid cooling to room temperature. This morphology is characteristic of polymeric nematics. In conclusion, the nematic structure of the liquid crystal phase appears to be sufficiently well assessed for all polymers.

Nickel-Containing Polymers. The polymers of this series show ^{1}H NMR spectra in agreement with the assigned formulas. In Table 2 some significant resonances are reported for P12-9NNi, as an example. Molecular weights are generally lower than those of the palladium-containing homologues. This feature may be argued from the intrinsic viscosity values (Table 2). Nonetheless, an average molecular weight of 6000 was measured by vapor pressure osmometry for the polymer showing the minimum value of intrinsic viscosity (P12-8NNi).

X-ray diffraction analysis shows that as-prepared polymers, with the exception of P12-12NNi, are noncrystalline at room temperature. All of them show LC mesomorphism. For $m = 8$, 9, and 10, the first DSC heating curve shows an exothermal transition, attributable to crystallization, peaked at 155, 120, and 140 °C, respectively, followed by the melting endotherm, whose maximum temperatures are reported in Table 4. On cooling, a large supercooling of the mesophase occurs,

Figure 6. X-ray diffraction pattern recorded at room temperature for a melt-extruded fiber of P12-9NPd.

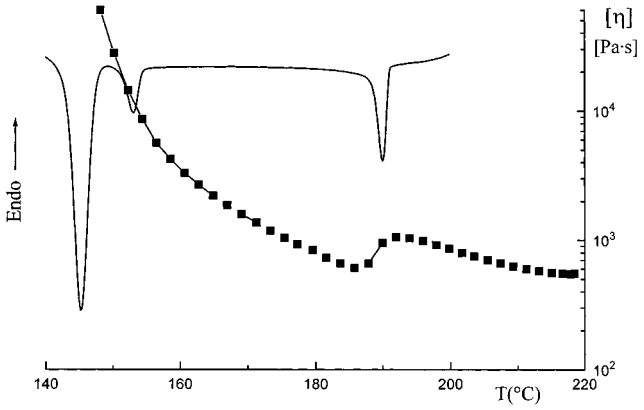

Figure 7. Melt viscosity (■) as a function of the temperature of the polymer P12-12NNi. Continuous line: DSC cooling cuve.

which may be detected at room temperature by X-ray diffraction means. The same holds for melt-extruded fibers, whose X-ray diffraction spectra recorded at room temperature are indicative of a cybotactic nematic phase. Figure 6 reports the diffraction pattern of a fibrous sample of P12-9NNi. It is characterized by an equatorial halo, centered at sin $\theta/\lambda = 0.116$ Å^{-1}, and by an intense but rather diffuse "four-spot pattern" at sin $\theta/\lambda = 0.0233$ Å^{-1}.

For polymer P12-11NNi, a DSC endothermic signal, which may be assigned to melting, is detectable in the first heating run notwithstanding the noncrystalline structure of the starting material and the absence of a previous sharp exothermic effect traceable to crystallization. Seemingly, crystallization must take place on heating within a large temperature range. Both P12-11NNi and P12-12NNi show monotropic nematic mesomorphism. This feature is suggested by the dependence on temperature of the melt viscosity curve (shown in Figure 7 for P12-12NNi) and by the DSC behavior (Figures 7 and 8).

Figure 8 reports how the nematic phase shows up on cooling the isotropic liquid and how the reverse transition may clearly be detected due to the kinetic retardation of the crystallization. The cooling curve shows also a low-enthalpy signal very likely related to the occurrence of liquid-crystalline polymorphism. However, the incoming crystallization frustrated any effort to define the structure of the presumably smectic phase.

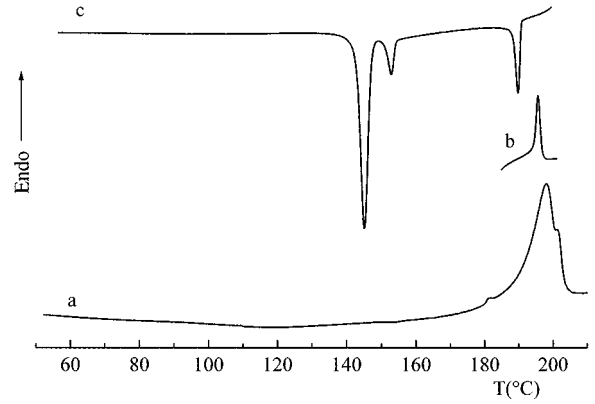

Figure 8. DSC curves for polymer P12-12NNi: scan rate, 10 °C/min; (a) first heating run; (b) second heating run after cooling at 170 °C; (c) first cooling run.

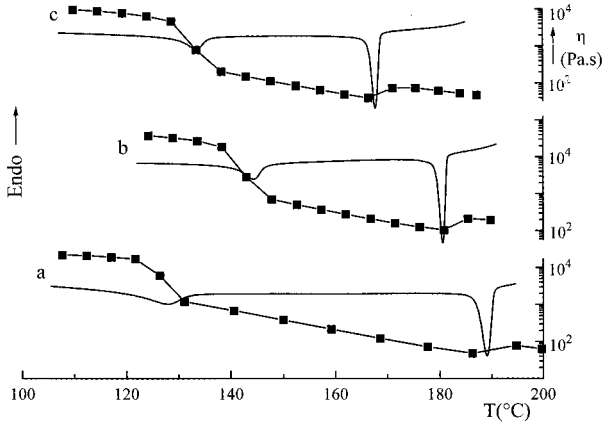

Figure 9. Dynamic melt viscosity as a function of temperature (■) superimposed on the DSC cooling curve: (a) P12-6NVO; (b) P12-8NVO; (c) P12-10NVO.

Table 5. Thermodynamic Data for Polymers P12-*m*NVO[a]

m	T_g	T_l	H_l	T_i	H_i	[η]
6	113	141	3.3	197	4.6	0.31
8	93	150	1.8	186	4.5	0.33
10	83	141	1.7	175	4.7	0.39

[a] T_g = glass transition temperature (°C); T_l = liquid−liquid transition temperature (°C); ΔH_l = liquid−liquid transition enthalpy (Jg^{-1}); T_i = isotropization temperature (°C); ΔH_i = isotropization enthalpy (J g^{-1}); [η] = limit viscosity number (dL g^{-1}) in chloroform at 25.0 °C.

Oxovanadium-Containing Polymers. Polymers of this series show enantiotropic liquid-crystalline polymorphism. The high-temperature liquid-crystalline phase has been recognized to be nematic. In fact, the X-ray diffraction pattern, recorded at the appropriate temperature, exhibits only a diffuse equatorial halo centered at sin $\theta/\lambda = 0.115$ Å^{-1}.

Moreover, as can be seen in Figure 9, the dynamic viscosity curves recorded at decreasing temperature in the range 200−130 °C show for all polymers a decrease of viscosity around the temperature at which an exothermic DSC signal indicates the transition from the isotropic liquid to the liquid-crystal phase. This is typical of the formation of a nematic structure.

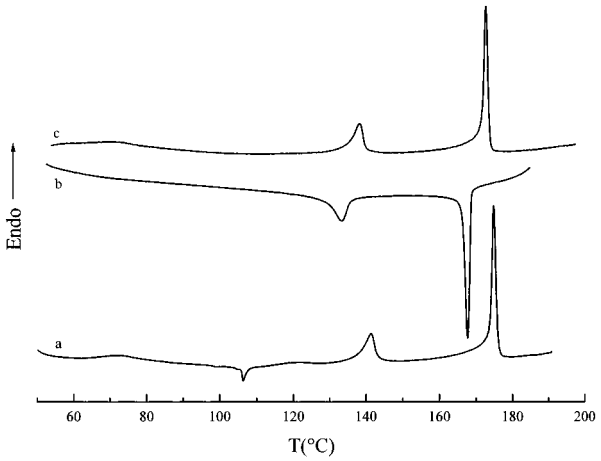

Figure 10. P12-10NVO. DSC curve recorded at a 10 °C/min scan rate: (a) first heating cycle; (b) first cooling cycle; (c) second heating cycle.

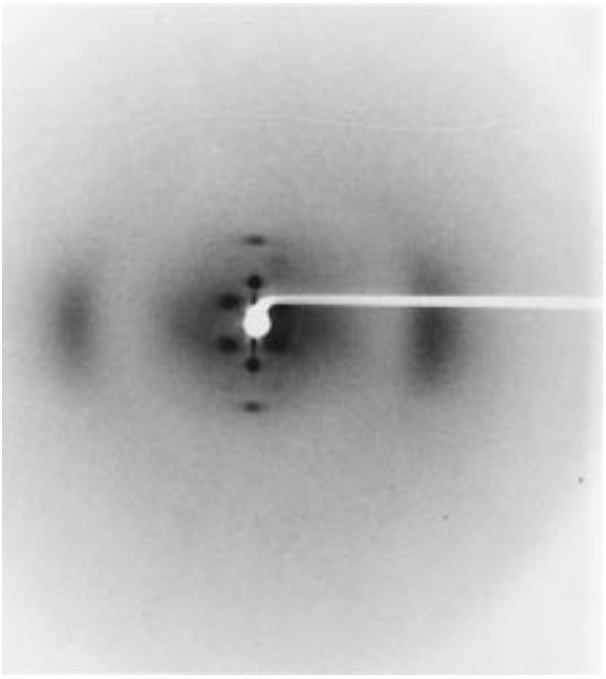

Figure 11. X-ray diffraction pattern of a fiber of P12-10NVO recorded at room temperature.

The DSC behavior of the polymers is substantially uniform (calorimetric data are reported in Table 5). It will be discussed for P12-10NVO, taken as an example, with reference to Figure 10.

In the first heating run (curve a), the glass transition is detectable at about 70 °C (cf. 83 °C by DMTA). An exothermic signal appears at 110 °C, with a very small enthalpic value. The origin of this phenomenon, which occurs only for previously untreated samples and is not accompanied by any structural change detectable by X-ray diffraction means, is not understood. The endothermic signal at 141 °C, on the basis of the optical observations, as well as of X-ray diffraction evidences, has been recognized as related to a liquid−liquid transition rather than to melting. The second endothermic peak, at 175 °C, corresponds to the isotropization. In the following cooling run, two exothermic signals indicate the reverse transitions, which correspond (Figure 9) respectively to a decrease and to an increase in the melt viscosity.

For all polymers, the X-ray diffraction pattern recorded at room temperature for fibrous or previously untreated samples indicates that no crystallinity is present. The only equatorial diffraction observed is a diffuse halo centered at $\sin\theta/\lambda = 0.116$ Å^{-1}. Annealing treatments at different temperatures lower than T_l (Table 5) were uneffective in producing crystallization. For all polymers, the X-ray diffraction pattern of a fibrous sample is further characterized by a strong and sharp meridian Bragg diffraction corresponding to a lattice distance of 17.7 ± 0.3 Å. The corresponding second-order diffraction is also detectable with a relative intensity increasing with m. The meridian diffractions are no longer observable at temperatures higher than T_l, consistent with the nematic structure of the high-temperature mesophase. The X-ray diffraction pattern of P12-10NVO (Figure 11) shows also a set of four sharp spots, symmetrically related, corresponding to a lattice distance of 23.2 ± 0.3 Å. An analogous feature, although considerably diffuse, is present also in the diffraction pattern of fibrous P12-8NVO while it is not detectable for P12-6NVO.

The diffraction data indicate for all polymers that the low-temperature mesophase is a smectic phase lacking structural order across the smectic axis. The periodicity along the fiber axis, equal for all polymers within the experimental uncertainty, closely corresponds to half the length of the monomer unit calculated from literature data[15] in its most extended conformation. This implies an intercalation of the polymer chains with an average relative shift along the smectic axis equal to half the monomer unit length. For m = 6 and 8, the smectic phase should be of S_A type, possibly with some cybotactic distortion particularly for m = 8. For m = 10, the presence of sharp nonequatorial and nonmeridian Bragg diffractions makes any decision about the mesophase structure less straightforward. If the "four-spot pattern" is taken into account (independently) as indicative of chain tilting with respect to the smectic periodicity (as for a S_C smectic), a tilt angle of 48 ± 1.5° is calculated with a smectic periodicity of 34.9 ± 0.5 Å, which is consistent with the length of the monomer unit.

Table 6. Comparison of Thermodynamic Data for P12-*m*NM Homologues: M = VO, Cu, Ni, Pd[a]

	T_m				T_i				ΔH_i			
m	VO	Cu[b]	Ni	Pd	VO	Cu[b]	Ni	Pd	VO	Cu[b]	Ni	Pd
6					197				4.6			
8		182	197	210	186	196	216	250	4.5	5.4	5.6	4.8
9		184	210	212		194	214	246		5.9	5.7	4.8
10		187	155	180	141	186	206	227	4.7	5.8	5.5	4.4
11		194	197	194		186	197	227		6.1	5.5	4.4
12		194	198			176	195				5.4	

[a] T_m = melting temperature (°C); T_i = isotropization temperature (°C); ΔH = isotropization enthalpy (J g^{-1}). [b] Thermodynamic data of copper-containing polymers are taken from ref 12.

In conclusion, for polymer P12-10NVO, the S_C (The occurrence of this structure was already observed in similar polymers[12] and in homologous low-molecular-weight compounds[16] where the smectic C phase takes over for longer lateral flexible chains.) and S_A arrangements might be present together or a small-enthalpy S_C-S_A phase transition might take place close to the smectic−nematic transition. However, it seems more likely that the smectic phase is of intercalated S_A type, as for P12-6NVO and P12-8NVO and that the sharpening of the "four-spot pattern" is related to a structure modulation across the chain axis operated for all polymers by the different steric bulk of the side chains.

In a critical review by Pasquali et al.,[15] it is reported that the characteristic geometry of bidentate Schiff base oxovanadium complexes is square-pyramidal, although the coordination geometry may also be distorted to trigonal bipyramidal. The liquid crystallinity of our polymers and the X-ray data related to the length of the monomer units are more consistent with a square-pyramidal coordination geometry which fits better the need for an elongated linear shape.

It has also been reported that a hexacoordination of V^{IV} is carried out by the interaction of the oxygen atom with another VO unity,[8,17] leading often to a V═O stretching vibration frequency lower than the value reported for the isolated oxovanadium entity (960 ± 50 cm^{-1}).[18] The oxovanadium stretching frequency measured for P12-*m*NVO is 984 cm^{-1}. This should exclude the presence of strong interactions and is consistent with the intercalated packing model for the smectic phase.

Conclusion

For a conclusive comparison of the entire set of Cu-, Ni-, Pd-, and VO-containing homologues, melting and isotropization data are summarized in Table 6. From these data it is evident that the stability of the nematic phase follows the trend Pd > Ni > Cu > VO for any value of *m*. Following, although in a less clear-cut way, a general trend observed among main chain liquid-crystalline polymers containing lateral substituents, the liquid-crystalline phase stability decreases with increasing length (and bulk) of the flexible substituent. Although melting temperatures may not be entirely comparable due to possibly different thermal histories, the stability interval of the mesophase decreases along the sequence VO > Pd > Ni > Cu. A decreasing trend is also observable with increasing *m* in such a way that monotropism is mostly characterizing the copper complexes, with a T_i-T_m difference as low as −18 °C for $m = 12$, while all Pd- and VO-containing polymers are LC-enantiotropic. A further difference, concerning the phase behavior, is worthy of notice. For copper-containing polymers with $m > 9$ a monotropic mesophase, probably of smectic C type, was detected both by DSC and X-ray diffraction techniques; nothing of the like was found for Ni- and Pd-containing homologues, while all reported polymers containing the oxovanadium group show also a smectic phase in a seemingly (no melting temperature was measurable for these polymers) enantiotropic way. A stabilization of the smectic phase has been observed also for similar low-molecular-weight compounds.[19] For polymers, however, this difference may be not as drastic as it appears. In fact, for P12-10NCu, a smectic C phase is monotropically detectable below ∼100 °C and the enantiotropism observed for the smectic phase of P12-10NVO might be due to its poor crystallizability. Anyhow, although the mesophase stability interval is practically the largest for vanadium-containing polymers, the absolute stability is the lowest. Both effects are probably connected to some distortion of the mesogen linearity and to an increase of its average cross-section produced by the VO-coordinated group. Finally, isotropization enthalpies are scarcely dependent on *m* but show a decreasing trend along the sequence Cu > Ni > Pd ∼ VO. A similar feature had already been observed for low-molecular-weight analogues.[18] It is possible that differences in the liquid crystalline properties connected to the nature of the coordinated metal atom may be related to structural diversities in the coordination geometry: strictly square-planar for Pd complexes, more or less tetrahedrally distorted for those containing Ni or, particularly for those containing Cu, and square-pyramidal for VO complexes. However, this relationship has not been demonstrated as yet.

Acknowledgment. This research was supported by Ministero dell'Università e della Ricerca Scientifica e Tecnologica. The authors are grateful to Prof. M. Acierno and Dr. M. E. Frigione for dynamic viscosity measurements. NMR spectra were recorded at the "Centro Interdipartimentale di Metodologie Chimico Fisiche".

References and Notes

(1) Oriol, L.; Serrano, J. L. *Adv. Mater.* **1995**, *7*, 348.

(2) Hanabusa, K.; Tanimura, Y.; Suzuki, T.; Koyama, T.; Shirai, H. *Makromol. Chem.* **1991**, *192*, 233.

(3) Hanabusa, K.; Suzuki, T.; Koyama, T.; Shirai, H. *Makromol. Chem.* **1992**, *193*, 2149.

(4) Onitsuka, K.; Ogawa, H.; Joh, T.; Takahashi, S. *Chem. Lett.* **1988**, 1855.

(5) Chen, G.; Zhang, R. *Chin. J. Polym. Sci.* **1991**, *9*, 339.

(6) Caruso, U.; Roviello, A.; Sirigu, A.; Troise, C. *New Polym. Mater.* **1996**, *5*, 1.

(7) Wilkinson, G., Gillard, R. D., McCleverty, J. A., Eds. *Comprehensive Coordination Chemistry*; Pergamon Press: Oxford, 1987.

(8) Serrette, A.; Carroll, P. J.; Swager, T. M. *J. Am. Chem. Soc.* **1992**, *114*, 1887.

(9) Bikchantev, I.; Galyametdinov, Yu.; Prosvirin, A.; Griesar, K.; Soto-Bustamante, E. A.; Haase, W. *Liq. Cryst.* **1995** *18* (2), 231.

(10) Zheng, H.; Carroll, P. J.; Swager, T. M. *Liq. Cryst.* **1993**, *14* (5), 1421.

(11) Alonso, P. J.; Martinez, J. I.; Oriol, L.; Pinõl, M.; Serrano, J. L. *Adv. Mater.* **1994**, *6* (9), 663.

(12) Caruso, U.; Roviello, A.; Sirigu, A. *Macromolecules* **1991**, *24*, 2606.

(13) Griffin, A. C.; Havens, S. J. *J. Polym. Sci., Polym. Phys. Ed.* **1981**, *19*, 951.

(14) Buglione, J. A.; Roviello, A.; Sirigu, A. *Mol. Cryst. Liq. Cryst.* **1984**, *106*, 169.

(15) Pasquali, M.; Marchetti, F.; Floriani, C.; Merlino, S. *J. Chem. Soc., Dalton Trans.* **1977**, 139.

(16) Caruso, U.; Roviello, A.; Sirigu, A. *Liq. Cryst.* **1991**, *10* (1), 85.

(17) Mathew, M.; Carty, A. J.; Palenik, G. J. *J. Am. Chem. Soc.* **1970**, *92*, 3197.

(18) Farmer, R. L.; Urbach, F. L. *Inorg. Chem.* **1974**, *13*, 587.

(19) Blake, A. B.; Chipperfield, J. R.; Hussain, W.; Paschke, R.; Sinn, E. *Inorg. Chem.* **1995**, *34*, 1125.

MA970187N